

## Supplemental table

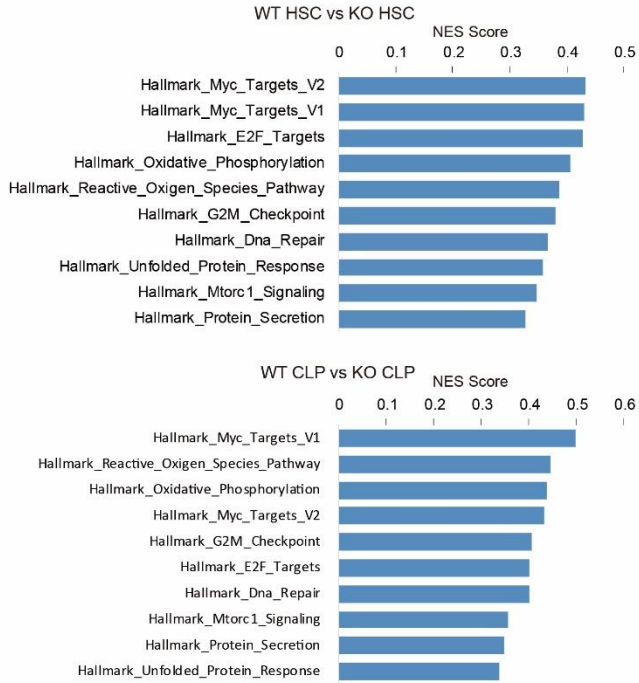
**Table S1 Oligos used in realtime-PCR experiments.**

Gene	Species	Forward	Reverse
<i>Grk6</i>	hsa	AGCGTGACTATCACAGCCTG	CTTCCGCTTGTCATCCGGG
<i>Rpl13a</i>	hsa	CCAAGCGGCTGCCGAAGATGG	CTTCCGGCCCAGCAGTACCTGT
<i>Nox2</i>	mmu	CTGAAGGGGGCCTGTATGTG	CCAAACTCTCCGCAGTCTGT
<i>Nox4</i>	mmu	TGTTGGGCCTAGGATTGTGT	CAGGACTGTCCGGCACATAG
<i>Cdkn1a</i>	mmu	TCAGGCGCAGATCCACAGCG	CGAACGCGCTCCCAGACGAA
<i>Sod3</i>	mmu	GAGCTCTTGGGAGAGCCTGA	GCTCCATCCAGATCTCCAGC
<i>Nox1</i>	mmu	CCTGATTCCTGTGTGTCGAAA	TTGGCTTCTTCTGTAGCGTTC
<i>Gapdh</i>	mmu	TGTGTCCGTCGTGGATCTGA	CCTGCTTCACCACCTTCTTGA
<i>Sod1</i>	mmu	ATGGCGATGAAAGCGGTGT	CAGTCACATTGCCAGGTCT
<i>Sod2</i>	mmu	TTCTGGACAAACCTGAGCCC	GTCACGCTTGATAGCCTCCA
<i>Grk6</i>	mmu	TTCCCCATATCAGCCAGTGT	CGTAGCACAGAACTCACGAAAT
<i>Nrf2</i>	mmu	TCTTGGAGTAAGTCGAGAAGTGT	GTTGAAACTGAGCGAAAAAGGC

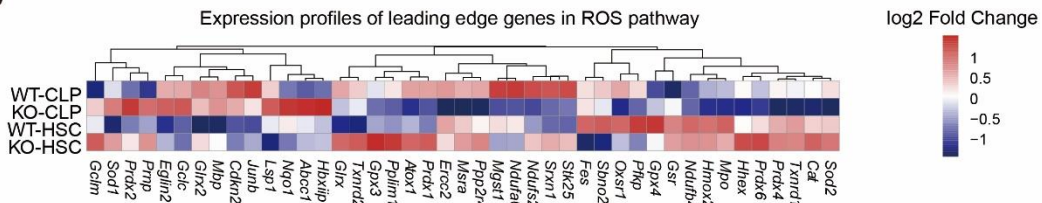
# Supplemental data

## Figure S1

a



b



c

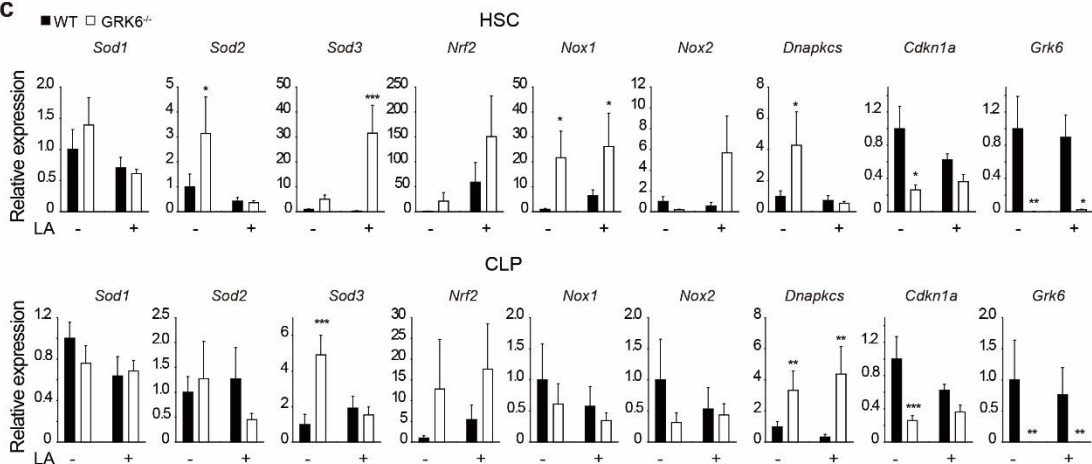


**Figure S1. GRK6 ablation leads to alterations in ROS pathway.** (a) Top ten significantly changed hallmark pathways in HSC and CLP caused by GRK6 ablation. (b) Expression profiles

of leading edge genes in ROS pathway were presented. (e) Real-time PCR quantification of *Sod1*, *Sod2*, *Sod3*, *Nrf2*, *Nox1*, *Nox2*, *Dna-pkcs*, *Cdkn1a*, *Grk6* (WT + Saline, WT + LA, GRK6<sup>-/-</sup> + Saline, GRK6<sup>-/-</sup> + LA, N = 5, 4, 3, 3). Two-way ANOVA with Bonferroni *post hoc*; \*  $P < 0.05$ , \*\*  $P < 0.01$ , \*\*\*  $P < 0.001$ , within genotype. Data are expressed as Mean  $\pm$  SEM.

## Figure S2

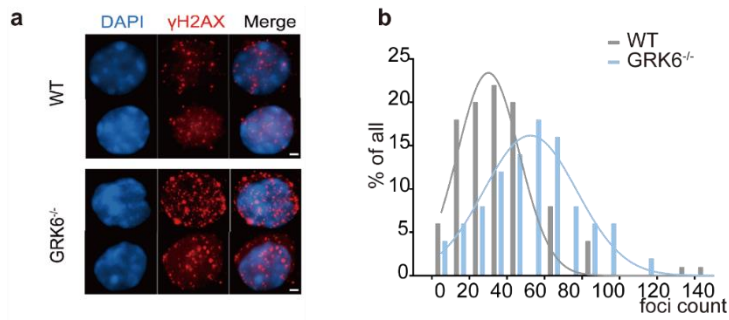


**Figure S2. More  $\gamma$ -H2AX foci in GRK6<sup>-/-</sup> than WT HSC.** Sorted cells were stained for intracellular  $\gamma$ -H2AX using phospho-specific antibody, and photographed by confocal microscopy. Foci of  $\gamma$ -H2AX positive dots from 100 cells were counted in each population. (a) Representative immunofluorescence graphs. Objective, Plan-Apochromat 63 $\times$ /1.4. Scale Bar, 2  $\mu$ m. (b) Plot of distribution.  $t(198) = 3.138$ ,  $p = 0.002$ , two-tailed, unpaired Student's  $t$ -test.

## Figure S3

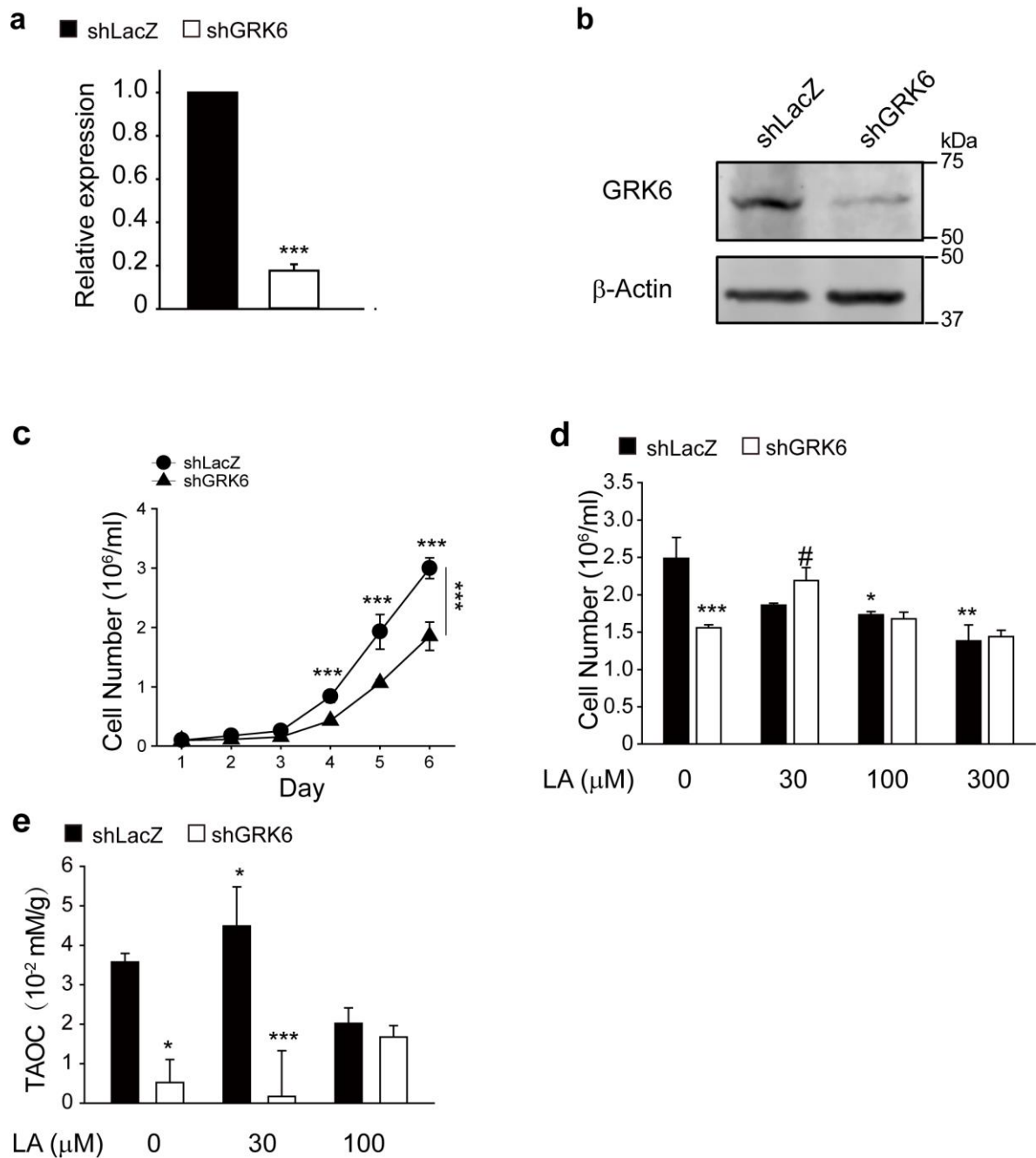


**Figure S3. GRK6 knockdown leads to growth arrest and reduced antioxidative capacity.**

(a-b) GRK6 knockdown efficiency was tested, (a) in HEK293T by RT-PCR, and (b) in Jurkat by Western blot. (c) GRK6 knockdown lead to reduced cellular growth. Seventy two hours after lentiviral spinoculation,  $2 \times 10^5$ /ml Jurkat cells were cultured in RPMI 1640 supplemented with 10% FBS and cellular density was measured daily.  $F_{\text{virus} \times \text{day}} = 7.141$ ,  $P < 0.001$ . (d) LA

improved cell growth in lentivirus-mediated GRK6 knockdown.  $F_{\text{virus} \times \text{dose}} = 6.746, P = 0.004$ .

(e) LA was supplied to cell culture media and TAOC was measured 6 hr later. Two-way ANOVA with Bonferroni post hoc. \*  $P < 0.05$ , \*\*\*  $P < 0.001$ , within genotype; #  $P < 0.05$  within treatment.  $N = 4$  each. Data are expressed as Mean  $\pm$  SEM.

## Figure S4

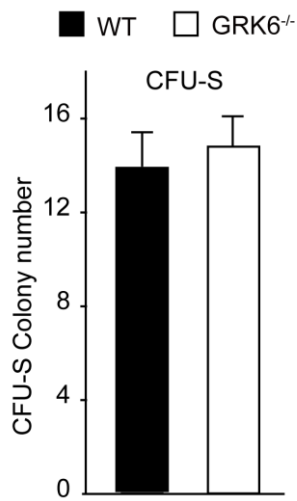


**Figure S4. GRK6 is dispensable in migration and short-term reconstitution of hematopoietic progenitor cells.** Spleen clonogenic (CFU-S) assay.  $5 \times 10^5$  bone marrow cells from GRK6<sup>-/-</sup> or WT mice were retro-orbital injected into wild type recipient mice. Spleen was dissected at day 12 and enumerated for colonies (Recipients N = 5-6 each, donor N = 3 per group).